Electrodisintegration of ^{4}He Studied with the Reaction ^{4}He$(e,e'p)^3$H

J. F. J. van den Brand,[1] H. P. Blok,[1,2] R. Ent,[1,2] E. Jans,[1] G. J. Kramer,[1] J. B. J. M. Lanen,[3] L. Lapikás,[1] E. N. M. Quint,[1] G. van der Steenhoven,[1,2] P. K. A. de Witt Huberts[1,3]

[1]*Nationaal Instituut voor Kernfysica en Hoge Energiefysica (NIKHEF-K), 1009 AJ Amsterdam, The Netherlands*

[2]*Natuurkundig Laboratorium, Vrije Universiteit, Amsterdam, The Netherlands*

[3]*Fysisch Laboratorium, Rijksuniversiteit Utrecht, Utrecht, The Netherlands*

(Received 13 November 1987)

The coincidence cross section for the two-body breakup of ^{4}He has been determined up to recoil momenta of 350 MeV/c with the $(e,e'p)$ reaction. The momentum probability distribution for the $t+p$ final state deduced from the cross section is compared to theoretical predictions that include correlations. A substantial deviation from the impulse approximation is observed, which cannot fully be explained by final-state interaction effects and contributions due to charge exchange.

PACS numbers: 25.30.Fj, 21.30.+y, 27.10.+h

The two- and three-nucleon systems ^{2}H, ^{3}H, and ^{3}He have been intensively studied because one can, starting from a nucleon-nucleon (NN) interaction, in principle, calculate their properties exactly. Recently theoretical progress has been made[1-4] for ^{4}He in solving the corresponding four-body Schrödinger equation with various approximation schemes. In some of these calculations a three-nucleon interaction (TNI) is included in the Hamiltonian. Microscopic theory of correlated many-body systems predicts that short-range and tensor correlations play an important role in the compact four-nucleon system. The presence of correlations is expected to be manifest in the single-nucleon spectral function. Therefore accurate data for the quasielastic proton-knockout reaction ^{4}He$(e,e'p)$ for large missing-momentum and missing-energy ranges may provide a critical test of such microscopic theories.

The static properties of ^{4}He such as the binding energy and the charge distribution have been measured very accurately.[5] Only one study of the reaction ^{4}He$(e,e'p)$ is known[6] in which the proton momentum distribution has been measured up to 250 MeV/c with limited statistical accuracy. The missing-energy resolution (ΔE_m =9–15 MeV) did not permit a separation of the two-body breakup ^{4}He$(e,e'p)^3$H from the three- and four-body breakup processes $(e,e'p)^2$Hn and $(e,e'p)npn$. In this Letter we present spectral-function data extracted from precise absolute cross sections for the reaction ^{4}He$(e,e'p)^3$H measured with good missing-energy resolution (ΔE_m =0.3–1.2 MeV) as a function of recoil momentum in the range $10<p_m<350$ MeV/c.

The experiment was performed with the electron-scattering facility at NIKHEF-K[7] at an incident electron energy of 426 MeV. A cryogenic target system at an operating temperature of 20 K was employed.[8] The pressure of the ^{4}He gas was 400 kPa resulting in a luminosity of 1250 μA mg/cm^2, given the 5-cm maximum length of the interaction region observed in the coincidence measurements. Data were taken under two different kinematical conditions, with the relative kinetic energy of the proton-triton pair in the center-of-mass system kept constant at 75 MeV. In the first kinematics (I) the electron scattering angle was 70°, the virtual-photon polarization ϵ=0.48, and the transferred three-momentum $|q|$ =431 MeV/c. The missing-momentum range $10<p_m<200$ MeV/c was covered by variation of the proton-emission angle θ_p relative to the electron beam in the range $47°<\theta_p<68°$. The second kinematics (II) with θ_e =36° and ϵ =0.80 covered the missing-momentum range $120<p_m<350$ MeV/c ($58°<\theta_p<118°$). Here $|\mathbf{q}|$ =250 MeV/c was chosen in order to compensate for the decrease of the spectral function with increasing momentum. Note that kinematics I corresponds to so-called perpendicular kinematics,[9] whereas kinematics II is strictly parallel for p_m centered around 135 MeV/c. At p_m =160 MeV/c, where the center of the overlap region between kinematics I and II is located, the angle between $\mathbf{q}$ and the initial proton momentum $\mathbf{p}$ amounts to 105° (46°) for kinematics I (II).

The product of the target thickness and the solid angle of the electron spectrometer was determined by comparison of the measured elastic electron-scattering cross section with the phase-shift calculations using ground-state charge-distribution parameters from the literature.[5] For each coincidence setting the target thickness, which varied as a function of the power dissipated in the target cell by at most 28%, could be related within an accuracy of 2% to the results of the elastic electron experiments by use of the corresponding proton singles rates. As an additional check on the relative normalization of kinematics I and II, we measured the elastic electron-scattering cross section at the forward and backward electron spectrometer angles, respectively, using the proton spectrometer as a target thickness monitor at a fixed angle and fixed magnetic-field setting. The ratio of the target densities at these two angles determined from the elastic electron-scattering cross sections was consistent with the ratio of the proton singles rates within the statistical ac-

curacy of 2%.

The coincidence-detection efficiency was calibrated repeatedly with the reaction ^{1}H$(e,e'p)$; it amounted to 99.2(1.3)%. The total ^{4}He$(e,e'p)$ yield was corrected for accidental coincidences and weighted by the detection volume calculated with a Monte Carlo simulation, taking the experimentally determined angular acceptance of the spectrometers as a function of the interaction point into account. Radiative tails were unfolded and corrections were made for dead-time effects ($<17\%$).

The stability of the experimental apparatus was checked by our taking two data sets at the same kinematical setting, $p_m = 140$ MeV/c and $\theta_e = 36°$, at the beginning and end of the two-week run. The measured cross sections were found to be equal within the 2.8% statistical accuracy.

The total systematic error of 6% is obtained as follows. It consists of the quadratic sum of the uncertainties in the effective solid angles of the electron (1%) and proton spectrometers (3%), the coincidence detection efficiency (1.3%), and the target thickness. The last one is the linear sum of the systematical error of 2% quoted in the literature for elastic cross sections,[5] the 1% error due to the uncertainty in electron energy, and the statistical errors in the electron singles rates, which are smaller than 2.2% (0.7%) for kinematics I (II).

With use of the two high-resolution spectrometers and by application of the dispersion matching technique,[10] a missing-energy resolution of 390 keV was achieved at low p_m. At higher p_m the missing-energy resolution becomes worse, since the missing-momentum resolution of 5 MeV/c enters through the nonnegligible recoil term $p_m^2/2M_{A-1}$ in the expression for E_m.[9] A missing-energy (E_m) spectrum for $10 < p_m < 60$ Mev/c is shown in Fig. 1. In the observed excitation-energy region very little strength is seen in the many-particle breakup channels.

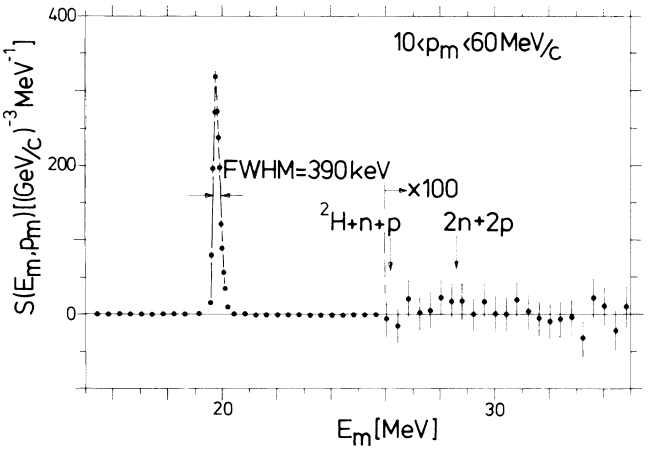

FIG. 1. Radiatively unfolded spectral function as a function of missing energy E_m measured in kinematics I at $\theta_p = 47°$. The arrows indicate the threshold energies for the $(e,e'p)^2$Hn and $(e,e'p)npn$ breakup channels.

In the plane-wave impulse approximation (PWIA)[9] the sixfold differential cross section is given by $d^6\sigma/de'd\mathbf{p}' = K\sigma_{ep}S(E_m,p_m)$. Here K denotes a kinematical factor, σ_{ep} describes the off-shell electron-proton scattering cross section, and the spectral function $S(E_m,p_m)$ contains the nuclear-structure information. The measured coincidence cross sections were converted to a spectral function by our dividing out $K\sigma_{ep}$ on an event-by-event basis. For σ_{ep} we used the current-conserving prescription σ_{f}^{cc} as given by de Forest.[11]

Integration of $S(E_m,p_m)$ over the two-body breakup peak at $E_m = 19.8$ MeV, corresponding to the residual (pnn) triplet in the triton ground state ($T = \frac{1}{2}$, $S = \frac{1}{2}$), yields the proton momentum density distribution $\rho(p_m)$ shown in Fig. 2. In the overlap region between kinematics I and II ($120 < p_m < 200$ MeV/c) the ratio of the momentum density distribution values is $\rho_{\text{I}}/\rho_{\text{II}} = 1.72 \pm 0.05$. In this ratio the systematic errors of the two kinematics cancel to a large extent. We will first discuss the observed deviation from unity in the framework of the distorted-wave impulse approximation (DWIA).

The PWIA momentum distribution for the $t+p$ channel $\rho(p_m)$ as calculated by Akaishi[2] is represented in Fig. 2 by the solid curve. This author used the method

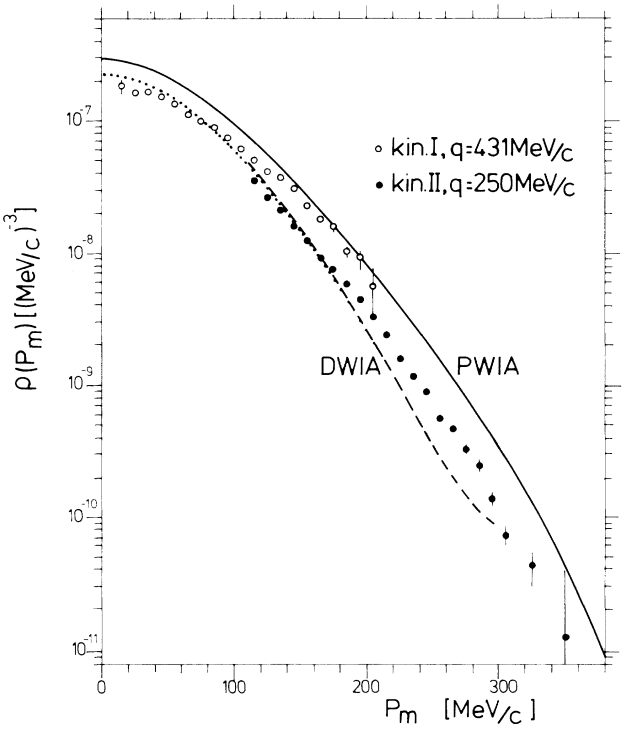

FIG. 2. Proton momentum distribution for the two-body breakup of ^{4}He. The error bars include the statistical error only. The solid curve represents a PWIA calculation of Akaishi (Ref. 2) for the Reid soft-core V8 NN potential. The dotted and dashed curves represent DWIA calculations for kinematics I and II, respectively.

of amalgamation of two-body correlations into multiple-scattering processes and the Reid soft-core V8 nucleon-nucleon interaction to which a TNI was added. When comparing the data with calculated momentum densities one has to account for final-state-interaction (FSI) effects, which depend on the choice of the kinematics. We performed an unfactorized[9] DWIA calculation using a $t+p$ ground-state wave function that reproduces the $\rho_{t+p}(p_m)$ of Akaishi, which accounts for 80% of the ^{4}He ground state. An optical potential including a spin-orbit term[12] was used to calculate the FSI effects. The DWIA results for both kinematics clearly fail to describe the full experimental shape of the momentum distributions, as can be observed in Fig. 2. Not only is the deviation of the experimental results in the overlap region not reproduced but also the slope of the DWIA results is incompatible with the experimental observations.

PWIA results calculated by Schiavilla, Pandharipande, and Wiringa[1] are shown in Fig. 3. These authors use a Monte Carlo method based on a realistic Hamiltonian, which includes a TNI, and variational wave functions, which have a pair-correlation operator including central, tensor, and spin correlations. In the figure the PWIA and DWIA $t+p$ momentum distributions are plotted for the Urbana NN potential. Since in kinematics I and II the relative kinetic (p-t) energy is the same, the difference in the DWIA results is also small. Good agreement between data and theory is obtained for kinematics II: $\rho_{\mathrm{II}}^{\mathrm{expt}}/\rho_{\mathrm{DWIA}}=0.98\pm0.09$. The error includes the systematical error and an error (7%) due to the uncertainty in the optical potential. However, for kinematics I the calculation yields values substantially smaller than the data: $\rho_{\mathrm{I}}^{\mathrm{expt}}/\rho_{\mathrm{DWIA}}=1.54\pm0.11$. Apparently FSI effects alone are not able to explain the discrepancy between the results obtained in kinematics I and II. The shape of the experimental momentum density distribution is in fair agreement with a correlated ^{4}He wave function[1] that was calculated with the Urbana NN potential.

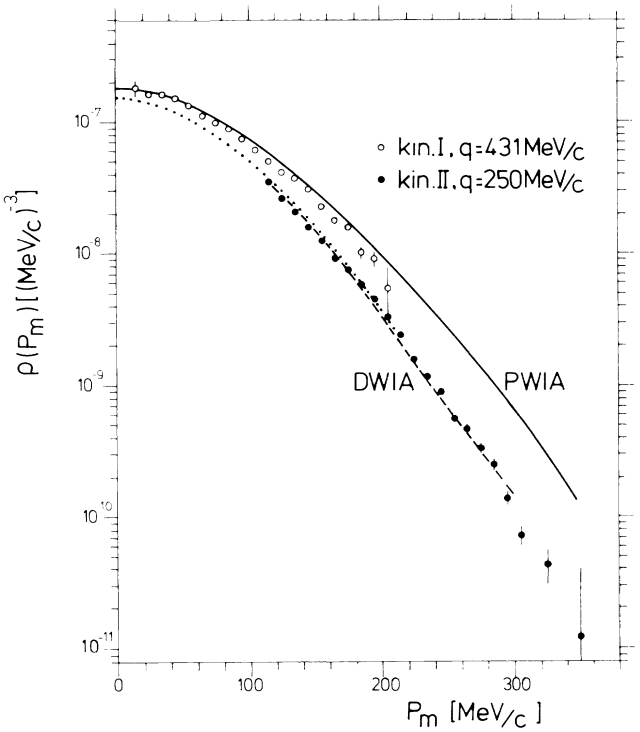

FIG. 3. The experimental proton momentum distribution for the two-body breakup of ^{4}He is the same as that given in Fig. 2. The solid curve represents a PWIA calculation of Schiavilla, Pandharipande, and Wiringa (Ref. 1), for the Urbana NN potential. The dotted and dashed curves represent corresponding DWIA calculations for kinematics I and II, respectively.

As a second step we will consider other effects which may influence the interpretation of the data. The contribution from the $(e,e'n)(n,p)$ two-step process was estimated by employment of a coupled-channels calculation in which a (p,n)-exchange potential was used reproducing the measured cross sections for the reaction ^{3}H$(p,n)^3$He at 57 and 156 MeV,[13,14] which are relatively strong compared to the elastic channel. Assuming isospin symmetry we obtain that in kinematics I charge exchange can account for about 8% of the cross section at low missing momentum, whereas the effect is 40% at $p_m=300$ MeV/c. This strong dependence of the effect on p_m can be understood by our noting that the charge-exchange potential causes essentially a p_m shift of $\rho(p_m)$.[15] Because of the shape of $\rho(p_m)$ the effect is larger at high p_m. In the center of the overlap region the contribution of charge exchange to the coincidence cross section amounts to 20%. For kinematics II the effect is much smaller and amounts to only 5% at $p_m=160$ MeV/c. If we take the charge-exchange contribution also into account, there remains a 40% discrepancy between the results obtained in kinematics I and II.

A similar but less pronounced signature for the deviation from the impulse approximation was found in several $(e,e'p)$ experiments,[16,17] performed in *parallel* kinematics only, where the observed effect can be described by our assuming an effective photon-proton coupling, that depends on the virtual-photon polarization ϵ. In the present experiment ϵ amounts to 0.48 and 0.80 for kinematics I and II, respectively. Therefore we have analyzed the data with an (18 ± 3)% modified ratio of transverse-longitudinal photon-proton coupling which has been deduced[17] from $1s$ knockout from ^{6}Li. Including the charge-exchange contribution, we then obtain $\rho_{\mathrm{I}}^{\mathrm{expt}}/\rho_{\mathrm{DWIA}}=1.12\pm0.13$ and for kinematics II $\rho_{\mathrm{II}}^{\mathrm{expt}}/\rho_{\mathrm{DWIA}}=0.89\pm0.08$. To what extent the still remaining deviation from the impulse approximation is caused by an incorrect prescription of σ_{ep}, by final-state-interaction effects beyond the DWIA, or by processes involving meson-exchange currents is not clear at present. Therefore a more conclusive test of the bound-state wave func-

tions has to await the availability of models capable of explaining the observed deviation.

This work is part of the research program of the National Institute for Nuclear Physics and High-Energy Physics (NIKHEF, section K), made possible by financial support from the Foundation for Fundamental Research on Matter (FOM) and The Netherlands' Organization for the Advancement of Scientific Research (ZWO).

[1]R. Schiavilla, V. R. Pandharipande, and R. B. Wiringa, Nucl. Phys. **A449**, 219 (1986).

[2]Y. Akaishi, Nucl. Phys. **A416**, 409c (1984).

[3]J. G. Zabolitzky and M. H. Kalos, Nucl. Phys. **A356**, 114 (1981).

[4]A. C. Fonseca, Nucl. Phys. **A416**, 421c (1984).

[5]J. S. McCarthy, I. Sick, and R. P. Whitney, Phys. Rev. C **15**, 1396 (1979).

[6]V. A. Goldstein *et al.*, Nucl. Phys. **A335**, 333 (1981).

[7]C. de Vries *et al.*, Nucl. Instrum. Methods **223**, 1 (1984).

[8]J. F. J. van den Brand *et al.*, Nucl. Instrum. Methods **A261**, 373 (1987).

[9]S. Frullani and J. Mougey, Adv. Nucl. Phys. **14**, 1 (1984).

[10]P. K. A. de Witt Huberts and L. Lapikás, in *Proceedings of the Workshop on Electron Rings for Nuclear Physics Research,* edited by J. O. Adler (University of Lund, Sweden, 1982).

[11]T. de Forest, Jr., Nucl. Phys. **A392**, 232 (1983).

[12]W. T. H. van Oers *et al.*, Phys. Rev. C **25**, 390 (1982).

[13]R. Darves-Blanc *et al.*, Nuovo Cimento Lett. **4**, 16 (1972).

[14]H. Langevin-Joliot *et al.*, Nucl. Phys. **A158**, 309 (1970).

[15]G. van der Steenhoven *et al.*, Phys. Lett. B **191**, 227 (1987).

[16]G. van der Steenhoven *et al.*, to be published.

[17]G. van der Steenhoven *et al.*, Phys. Rev. Lett. **58**, 1727 (1987).